International Journal of Computer Information Systems and Industrial Management Applications
ISSN 2150-7988 Volume 18(8s) 2026 pp. 582-596
https://doi.org/10.70917/ijcisim-2026-2737
Article

TESA sub-model of upper truncated Abid system of distributions: properties, empirical inferences and application to plasma concentration measurements of indomethacin

Salah H. Abid, Masa M. H. Taher

Mathematic Department, Mustansiriyah University, Baghdad, Iraq.
Corresponding author email: abidsalah@gmail.com

Abstract: Truncation models natural boundary conditions, such as maximum possible earthquake magnitudes, top speeds, or physical constraints, providing a more accurate, bounded range for modeling data. In this paper, we will present the upper truncated Abid system of distributions and study in detail one of its sub-models, which we will call from now on the TESA distribution. Most of the important theoretical properties of the TESA distribution will be derived, including Rényi entropy, Tsallis entropy, Extropy, and the Stress-strength model. A detailed experimental study to evaluate maximum likelihood estimates under different TESA distribution patterns will be conducted, along with an applied study of indomethacin plasma concentration measurements (in μg/mL). In the applied study, the TESA distribution was compared with five competing distributions according to various criteria, and it was concluded that the TESA distribution is the best suited to the application under consideration due to its superior practical properties.
Keywords: NA

1. Introduction

Upper truncated probability distributions better represent natural phenomena because real-world systems often have physical, biological, or structural upper limits that continuous, unbounded distributions inaccurately ignore. Many processes cannot exceed a certain maximum value, such as material strength, human lifespan, or structural constraints, which are better modelled by a distribution with a hard boundary (truncation) rather than a long tail tending to infinity. Many researchers have addressed this topic over the past years with theoretical and experimental details, in addition to practical applications. In 1984, Mittal dealt with estimating the parameters of truncated distributions [1], in 1989, Wingo introduced the left-truncated Weibull distribution [2], in 1994, Del Castillo proposed the singly truncated normal model [3], in 2020, Aldahlan et al. introduced the truncated Cauchy power family of distributions [4], in 2020 also, Abid and Jani introduced doubly truncated generalized gamma distribution and doubly truncated Generalized Invers Weibull distribution [5], in 2021, Abid and Kadhim introduced Doubly truncated exponentiated inverted gamma [6], in 2022, Abid and Jani studied doubly truncated generalized Gompertz distribution and doubly truncated Marshal-Olkin extended Uniform distribution [7], in 2024, Sen et al. discussed the truncated Versions of the Xgamma Distribution [8], in 2024 also, Gómez et al. dealt with New generalization of the truncated Gumbel distribution [9], in 2025 , El Gazar et al. dealt with the truncated Perk distribution [10], in 2026, El Gazar et al. studied the Truncated Transmuted Exponential Distribution [11], In 2026 also, Mohammed et al. introduced Right – truncated [0,1] exponential Rayleigh distribution [12].

It is logical to say that the probability distribution consisting of a mixture of distributions have a significant set of advantages; firstly it combines features from all the distributions that shared to its construction, in addition to containing more parameters, thus providing it with more patterns to handle different phenomena. Based on this, Abid (2023) proposed his system, which will ensure that our introduced system here have the same features mentioned

above since it is based on the same foundation as the Abid system. The probability density function (pdf) of Abid system (AS) for generating mixture distributions can be defined as follows [13],

$$f(x) = c\left(\sum_{i=0}^{p} \theta_i x^i\right) e^{-\beta x^d} \ , x > 0 \quad (1)$$

Where, $c = \frac{d}{\sum_{i=0}^{p} \theta_i \frac{\Gamma((i+1)/d)}{\beta^{(i+1)/d}}}$ and $MP_s = \frac{\theta_s \frac{\Gamma((s+1)/d)}{\beta^{(s+1)/d}}}{\sum_{i=0}^{p} \theta_i \frac{\Gamma((i+1)/d)}{\beta^{(i+1)/d}}}, s = 1,2, \dots, p$ is the mixing proportions.

Many well-known distributions are sub-models of Abid system [13].

2. Upper truncated Abid system of distributions

By using well known formulas $g(x) = f(x)/F(b)$ and $G(x) = F(x)/F(b)$, one can get the upper truncated Abid system (UTAS) which will contains a lot of probability distributions and mixture of them by using different values of system parameters. The pdf of UTAS of distributions (Shows the distribution of failure or death times) can be written as,

$$g(x) = \frac{d\left(\sum_{i=0}^{p} \theta_i x^i\right) e^{-\beta x^d}}{\sum_{j=0}^{p} \theta_j \beta^{-(j+1)/d} \gamma\left(\frac{j+1}{d}, \beta b^d\right)} \ , \ 0 < x < b \quad (2)$$

The related cumulative distribution function cdf (the probability of failure or death by time x) will be,

$$G(x) = \frac{\sum_{i=0}^{p} \theta_i \beta^{-(i+1)/d} \gamma\left(\frac{i+1}{d}, \beta x^d\right)}{\sum_{j=0}^{p} \theta_j \beta^{-(j+1)/d} \gamma\left(\frac{j+1}{d}, \beta b^d\right)} \ , \ 0 < x < b \quad (3)$$

Therefore, the survival function SF (the probability of survival beyond time x) and the revised hazard rate function RHRF (the instantaneous risk profile of the distribution) will be respectively,

$$S(x) = 1 - \frac{\sum_{i=0}^{p} \theta_i \beta^{-(i+1)/d} \gamma\left(\frac{i+1}{d}, \beta x^d\right)}{\sum_{j=0}^{p} \theta_j \beta^{-(j+1)/d} \gamma\left(\frac{j+1}{d}, \beta b^d\right)} \ , \ 0 < x < b \quad (4)$$

$$H_R(x) = \frac{d\left(\sum_{i=0}^{p} \theta_i x^i\right) e^{-\beta x^d}}{\sum_{j=0}^{p} \theta_j \beta^{-(j+1)/d} \gamma\left(\frac{j+1}{d}, \beta x^d\right)} \ , \ 0 < x < b \quad (5)$$

The rth crude moments function can be derives as follows,

$$E(X^r) = \frac{d \int_0^b \left(\sum_{i=0}^{p} \theta_i x^{i+r}\right) e^{-\beta x^d} dx}{\sum_{j=0}^{p} \theta_j \beta^{-(j+1)/d} \gamma\left(\frac{j+1}{d}, \beta b^d\right)}$$

By using the transformation $U = \beta X^d$, then $X = (U/\beta)^{1/d}$ and $\frac{dx}{du} = \frac{1}{d\beta}\left(\frac{u}{\beta}\right)^{1/d-1}$, we get

$$E(X^r) = \frac{d}{\sum_{j=0}^{p} \theta_j \beta^{-(j+1)/d} \gamma\left(\frac{j+1}{d}, \beta b^d\right)} \int_0^{\beta b^d} \left(\sum_{i=0}^{p} \theta_i (u/\beta)^{\frac{i+r}{d}}\right) e^{-\beta x^d} \frac{1}{d\beta}\left(\frac{u}{\beta}\right)^{1/d-1} du$$

$$= \frac{1}{\sum_{j=0}^{p} \theta_j \beta^{-(j+1)/d} \gamma\left(\frac{j+1}{d}, \beta b^d\right)} \sum_{i=0}^{p} \theta_i (1/\beta)^{\frac{i+r+1}{d}} \int_0^{\beta b^d} u^{(i+r+1)/d-1} e^{-u} du$$

$$= \frac{\sum_{i=0}^{p} \theta_i (1/\beta)^{\frac{i+r+1}{d}} \gamma\left(\frac{i+r+1}{d}, \beta b^d\right)}{\sum_{j=0}^{p} \theta_j \beta^{-(j+1)/d} \gamma\left(\frac{j+1}{d}, \beta b^d\right)} \quad (6)$$

So the characteristic function will be

$$\varphi_X(t) = E(e^{itX}) = \sum_{v=o}^{\infty} \frac{(it)^v}{v!} E(X^v)$$

$$= \sum_{v=o}^{\infty} \frac{(it)^v}{v!} \frac{\sum_{i=0}^{p} \theta_i (1/\beta)^{\frac{i+v+1}{d}} \gamma\left(\frac{i+v+1}{d}, \beta b^d\right)}{\sum_{j=0}^{p} \theta_j \beta^{-(j+1)/d} \gamma\left(\frac{j+1}{d}, \beta b^d\right)} \quad (7)$$

2.1 Rényi entropy, Tsallis *entropy* and Extropy

The Rényi and Tsallis entropies are considerable in ecology, quantum information and statistics as hand of diversity, where they can be used as a measure of fog. Extropy from the other hand is a notion touching the possibility for evolution and hold, working as the conceptual cross of entropy (disorder). Now, let us find the value of integration $I = \int_0^\infty g^\alpha(y)dy$,

$I = c_1 \int_0^b \left(\sum_{i=0}^p \theta_i x^i\right)^\alpha e^{-\alpha\beta x^d} dx$ where $c_1 = \left(\frac{d}{\sum_{j=0}^p \theta_j \beta^{-(j+1)/d}\, \gamma\left(\frac{j+1}{d}, \beta b^d\right)}\right)^\alpha$, then

$I = c_1 \int_0^b \sum_{i_1=0}^p \dots \sum_{i_\alpha=0}^p \theta_{i_1} \dots . \theta_{i_\alpha}\, x^{i_1+i_2+\dots+i_\alpha} e^{-\alpha\beta x^d} dx$

By using the transformation, U=$\alpha\beta X^d$, then $X = (U/\alpha\beta)^{1/d}$ and $dx = \frac{1}{d\alpha\beta}\left(\frac{u}{\alpha\beta}\right)^{1/d-1} du$

$I = c_1 \sum_{i_1=0}^p \dots \sum_{i_\alpha=0}^p \theta_{i_1} \dots . \theta_{i_\alpha} \int_0^b (u/\alpha\beta)^{\frac{i_1+i_2+\dots+i_\alpha}{d}} \frac{1}{d\alpha\beta}\left(\frac{u}{\alpha\beta}\right)^{1/d-1} e^{-u} du$

$= \frac{c_1}{d} \sum_{i_1=0}^p \dots \sum_{i_\alpha=0}^p \frac{\theta_{i_1} \dots . \theta_{i_\alpha}}{(\alpha\beta)^{\frac{i_1+i_2+\dots+i_\alpha+1}{d}}} \int_0^b u^{\frac{i_1+i_2+\dots+i_\alpha+1}{d}-1} e^{-u} du$

$= \frac{c_1}{d} \sum_{i_1=0}^p \dots \sum_{i_\alpha=0}^p \frac{\theta_{i_1} \dots . \theta_{i_\alpha}}{(\alpha\beta)^{\frac{i_1+i_2+\dots+i_\alpha+1}{d}}} \gamma\left(\frac{i_1+i_2+\dots+i_\alpha+1}{d}, \alpha\beta b^d\right)$

Then the Rényi entropy $R_\alpha = \frac{1}{1-\alpha} Ln\left(\int_0^\infty g^\alpha(y)dy\right)$, where α is real and $\alpha \neq 1$ is [14],

$$R_\alpha = \frac{1}{1-\alpha} Ln\left(\frac{c_1}{d} \sum_{i_1=0}^p \dots \sum_{i_\alpha=0}^p \frac{\theta_{i_1} \dots . \theta_{i_\alpha}}{(\alpha\beta)^{\frac{i_1+i_2+\dots+i_\alpha+1}{d}}} \gamma\left(\frac{i_1+i_2+\dots+i_\alpha+1}{d}, \alpha\beta b^d\right)\right) \quad (9)$$

The Tsallis entropy $T_\alpha = \frac{1}{\alpha-1}\left(1 - \int_0^\infty g^\alpha(y)dy\right)$, where α is real and $\alpha \neq 1$ is [15],

$$T_\alpha = \frac{1}{\alpha-1}\left(1 - \frac{c_1}{d} \sum_{i_1=0}^p \dots \sum_{i_\alpha=0}^p \frac{\theta_{i_1} \dots . \theta_{i_\alpha}}{(\alpha\beta)^{\frac{i_1+i_2+\dots+i_\alpha+1}{d}}} \gamma\left(\frac{i_1+i_2+\dots+i_\alpha+1}{d}, \alpha\beta b^d\right)\right) \quad (10)$$

The extropy measure for a non-negative random variable is [16], $E = -\frac{1}{2}\int_0^\infty g^2(x)\, dx$. By making $\alpha = 2$ in equation (8), we get,

$$E = -\frac{1}{2}\frac{c_1}{d} \sum_{i_1=0}^p \sum_{i_2=0}^p \frac{\theta_{i_1}\theta_{i_2}}{(\alpha\beta)^{\frac{i_1+i_2+1}{d}}} \gamma\left(\frac{i_1+i_2+1}{d}, 2\beta b^d\right) \quad (11)$$

2.2 The Stress-Strength model

Let Y and X be the strength and stress the random variables, independent of each other, follow respectively UTAS(θ_i^*, β^*, d^*, b) and UTAS(θ_i, β, d, b) ($i = 0,1, \dots, p-1$) then the Stress- strength model of IASD is,

$R = E\left(G_Y(x)\right) = \int_0^b g_X(x) G_Y(x) dx$

$= c_2 \int_0^b g_X(x) \sum_{i=0}^p \theta_i^* (\beta^*)^{-(i+1)/d^*} \gamma\left(\frac{i+1}{d^*}, \beta^* x^{d^*}\right) dx$,

Where $c_2 = \left(\sum_{j=0}^p \theta_i^* (\beta^*)^{-(i+1)/d^*} \gamma\left(\frac{i+1}{d^*}, \beta^* b^{d^*}\right)\right)^{-1}$, then

$R = c_2 \sum_{i=0}^p \theta_i^* (\beta^*)^{-(i+1)/d^*} \int_0^b g_X(x) \gamma\left(\frac{i+1}{d^*}, \beta^* x^{d^*}\right) dx$,

By using $(s,x) = \Gamma(s) \sum_{k=0}^\infty \frac{x^{k+s} e^{-x}}{\Gamma(s+k+1)}$,

$R = c_2 \sum_{i=0}^p \theta_i^* (\beta^*)^{-(i+1)/d^*} \int_0^b g_X(x) \sum_{k=0}^\infty \frac{\left(\beta^* x^{d^*}\right)^{k+\frac{i+1}{d^*}} e^{-\beta^* x^{d^*}}}{\Gamma(\frac{i+1}{d^*}+k+1)} dx$

$$R = c_2 \sum_{i=0}^{p} \theta_i^* (\beta^*)^{-(i+1)/d^*} \Gamma(\tfrac{i+1}{d^*}) \sum_{k=0}^{\infty} \frac{(\beta^*)^{k+\frac{i+1}{d^*}}}{\Gamma(\frac{i+1}{d^*}+k+1)} \int_0^b g_X(x)\, e^{-\beta^* x^{d^*}} x^{kd^*+i+1} dx$$

Since $e^{-\beta^* x^{d^*}} = \sum_{m=0}^{\infty} \frac{(-\beta^*)^m x^{md^*}}{m!}$, then

$$R = c_2 \sum_{i=0}^{p} \theta_i^* (\beta^*)^{-(i+1)/d^*} \Gamma(\tfrac{i+1}{d^*}) \sum_{k=0}^{\infty} \sum_{m=0}^{\infty} \frac{(-1)^m}{m!} \frac{(\beta^*)^{m+k+\frac{i+1}{d^*}}}{\Gamma(\frac{i+1}{d^*}+k+1)} \int_0^b g_X(x)\, x^{kd^*+md^*+i+1} dx$$

$$= c_2 \sum_{i=0}^{p} \theta_i^* (\beta^*)^{-(i+1)/d^*} \Gamma(\tfrac{i+1}{d^*}) \sum_{k=0}^{\infty} \sum_{m=0}^{\infty} \frac{(-1)^m}{m!} \frac{(\beta^*)^{m+k+\frac{i+1}{d^*}}}{\Gamma(\frac{i+1}{d^*}+k+1)} E(X^{(k+m)d^*+i+1})$$

$$= c_2 \sum_{i=0}^{p} \theta_i^* (\beta^*)^{-(i+1)/d^*} \Gamma(\tfrac{i+1}{d^*}) \sum_{k=0}^{\infty} \sum_{m=0}^{\infty} \frac{(-1)^m}{m!} \frac{(\beta^*)^{m+k+\frac{i+1}{d^*}}}{\Gamma(\frac{i+1}{d^*}+k+1)} \frac{\sum_{l=0}^{p} \theta_l (1/\beta)^{\frac{l+(k+m)d^*+i+2}{d}} \gamma\left(\frac{l+(k+m)d^*+i+2}{d}, \beta b^d\right)}{\sum_{j=0}^{p} \theta_j \beta^{-(j+1)/d} \gamma\left(\frac{j+1}{d}, \beta b^d\right)} \quad (12)$$

3. TESA distribution

As sub-model of upper truncated Abid system (UTAS) of distributions, we will analyze and discuss in depth the case of p=2 of UTAS. The resulting distribution will henceforth be called the TESA distribution. The pdf of TESA random variable is,

$$g(x) = \frac{d(\theta_0+\theta_1 x+\theta_2 x^2) e^{-\beta x^d}}{\theta_0 \beta^{\frac{-1}{d}} \gamma\left(\frac{1}{d}, \beta b^{-d}\right) + \theta_1 \beta^{\frac{-2}{d}} \gamma\left(\frac{2}{d}, \beta b^{-d}\right) + \theta_2 \beta^{\frac{-3}{d}} \gamma\left(\frac{3}{d}, \beta b^{-d}\right)} \quad , \quad 0 < x < b \quad (13)$$

Where, $\theta_0, \theta_1, \theta_2, \beta, d > 0$ and b $(0 < x < b)$ are the parameters of TESA distribution and $\gamma(.,.)$ is the lower incomplete gamma function.

The cumulative distribution function of TESA distribution is,

$$G(x) = \frac{\theta_0 \beta^{\frac{-1}{d}} \gamma\left(\frac{1}{d}, \beta x^{-d}\right) + \theta_1 \beta^{\frac{-2}{d}} \gamma\left(\frac{2}{d}, \beta x^{-d}\right) + \theta_2 \beta^{\frac{-3}{d}} \gamma\left(\frac{3}{d}, \beta x^{-d}\right)}{\theta_0 \beta^{\frac{-1}{d}} \gamma\left(\frac{1}{d}, \beta b^{-d}\right) + \theta_1 \beta^{\frac{-2}{d}} \gamma\left(\frac{2}{d}, \beta b^{-d}\right) + \theta_2 \beta^{\frac{-3}{d}} \gamma\left(\frac{3}{d}, \beta b^{-d}\right)} \quad , \quad 0 < x < b \quad (14)$$

The other functions can be found from the general formulas of the previous section.

The effect TESA distribution parameters can be discussed as follows; the weighting parameters control the polynomial component $\theta_0 + \theta_1 x + \theta_2 x^2$ and determine the local shape of the distribution, essentially closely the origin. Baseline Weight parameter θ_0 controls the intercept. High θ_0 relative to others forces the distribution to behave more like a standard Exponential model at $x \to 0$. The Linear Growth parameter θ_1 inserts a slope. It is main for shifting the peak of the distribution away from zero, often seen in unimodal (hump-shaped) patterns. The curvature parameter θ_2 allows for bimodality or heavy shoulders. In Bathtub hazard cases, θ_2 is usually the dominant factor that handles the wear-out phase at higher values of x. The scale parameter β works as the extension factor for TESA distribution. Rise β squeezes the distribution toward the left (shorter life or faster decay). This is ideal in rapid-cast drug case. Low β flattens and reaches the distribution toward the right. The shape parameter d is the Main controller for the Hazard Rate Function (HRF). If $d < 1$ generally produces decreasing hazard rates (DHR). The probability of an event failing drops over time (the infant mortality phase in reliability). If $d = 1$, the TESA distribution simplifies toward a more traditional weighted exponential form. If $d > 1$, forces Increasing Hazard Rates (IHR). It introduces a doubly accelerated decay, meaning as x increases, the likelihood of the event occurring grows exponentially. Intermediate d Interacting with the weighting parameters, this creates the complex Bathtub and Upside-down Bathtub (Unimodal) shapes by balancing the polynomial growth against the exponential decay. The upper boundary parameter b ensures that the cumulative probability reaches 100% at a specific point. In the TESA distribution, as x approaches b, the hazard rate often increases or stabilizes depending on the other parameters, making it perfect for modeling processes that must seal (like a drug being totally cleared from a system).

Based on the structure of the TESA distribution, here are the possible hazard rate patterns,

1. Monotone Increasing Hazard Rate (MIHR) occurs when $\boldsymbol{d} > \mathbf{1}$ and $\boldsymbol{\theta_2} > \boldsymbol{\theta_0}$. This provokes a wear-out stage where the probability of failure increases rapidly as $\boldsymbol{x}$ approaches the boundary $\boldsymbol{b}$. The pdf shifts weight toward the right and the hazard rate Starts low and curves upward, eventually spiking at $\boldsymbol{b}$.

2. Monotone Decreasing Hazard Rate (MDHR) occurs when $\boldsymbol{d} < \mathbf{1}$ and $\boldsymbol{\theta_0} \gg \boldsymbol{\theta_1}, \boldsymbol{\theta_2}$. This emulates infant mortality, where the risk is highest at the beginning and declines. The pdf is heavily skewed to the left (highest at $\boldsymbol{x} = \mathbf{0}$) and the hazard rate slopes downward before the final truncation spike.

3. Bathtub-Shaped (BSHR)) requires a low $\boldsymbol{d}$ to capture early high risk, combined with a strong $\boldsymbol{\theta_2}$ to capture late-life wear-out. The pdf is usually U-shaped or high at both boundaries and hazard rate decreases, stabilizes in a "useful life" valley, then increases toward $\boldsymbol{b}$.

4. Unimodal (Upside-down Bathtub) (UHR) occurs at Mid-range $\boldsymbol{d}$ (around 1.5–2) with $\boldsymbol{\theta_1}$ or $\boldsymbol{\theta_2}$ dominating to push the mode into the center of the interval $(\mathbf{0}, \boldsymbol{b})$. The pdf have Bell-shaped within the truncated range and hazard rate Increases to a peak risk and then decreases before the final boundary effect.

5. Constant Hazard Rate (CHR) occurs at $\boldsymbol{d} = \mathbf{1}$ and $\boldsymbol{\theta_1} = \boldsymbol{\theta_2} = \mathbf{0}$. This reduces the TESA distribution to a Truncated Exponential Distribution and the hazard rate will be Flat (horizontal) across the support until it hits the boundary $\boldsymbol{b}$.

Table (1) contains the values of the TESA distribution parameters according to which the pdf, cdf, sf and hazard rate function were plotted. The plots are in figure (1) under different patterns of TESA distribution.

Table (1): TESA distribution Parameters values according to which

pdf, cdf, sf and hazard rate function were plotted

Pattern	$\boldsymbol{\theta_0}$	$\boldsymbol{\theta_1}$	$\boldsymbol{\theta_2}$	$\boldsymbol{\beta}$	$\boldsymbol{d}$	$\boldsymbol{b}$	Description
MIHR	0.1	0.2	0.7	0.5	2.0	5	Strong aging effect ($d > 1$) and high-order weighting.
MDHR	0.9	0.05	0.05	2.0	0.5	5	Early failure dominance ($d < 1$) and constant-term weight.
BTHR	0.5	0.0	0.5	0.1	0.5	5	High risk at $x \to 0$ and $x \to b$ with a stable middle.
UHR	0.0	1.0	0.0	0.2	1.5	5	Risk peaks in the "mid-life" of the distribution.
CHR	1.0	0.0	0.0	1.0	1.0	5	Reduces to a Truncated Exponential distribution.

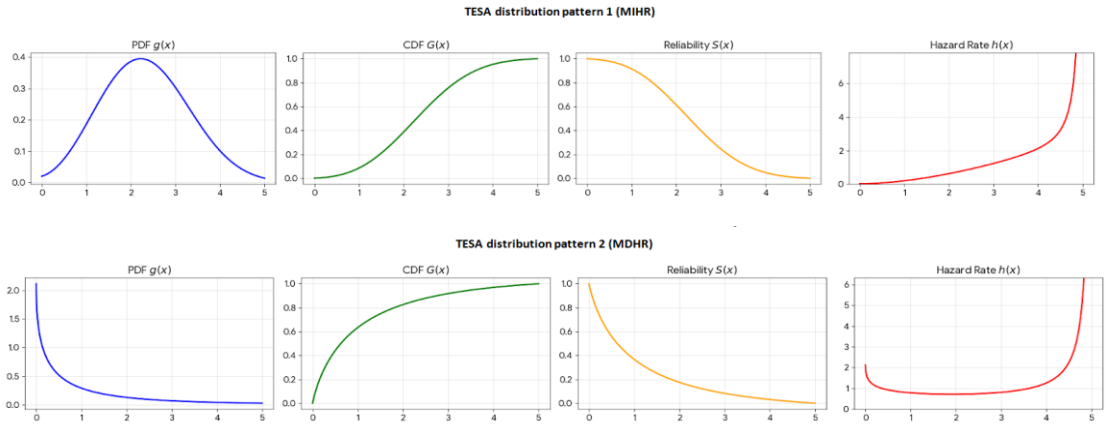

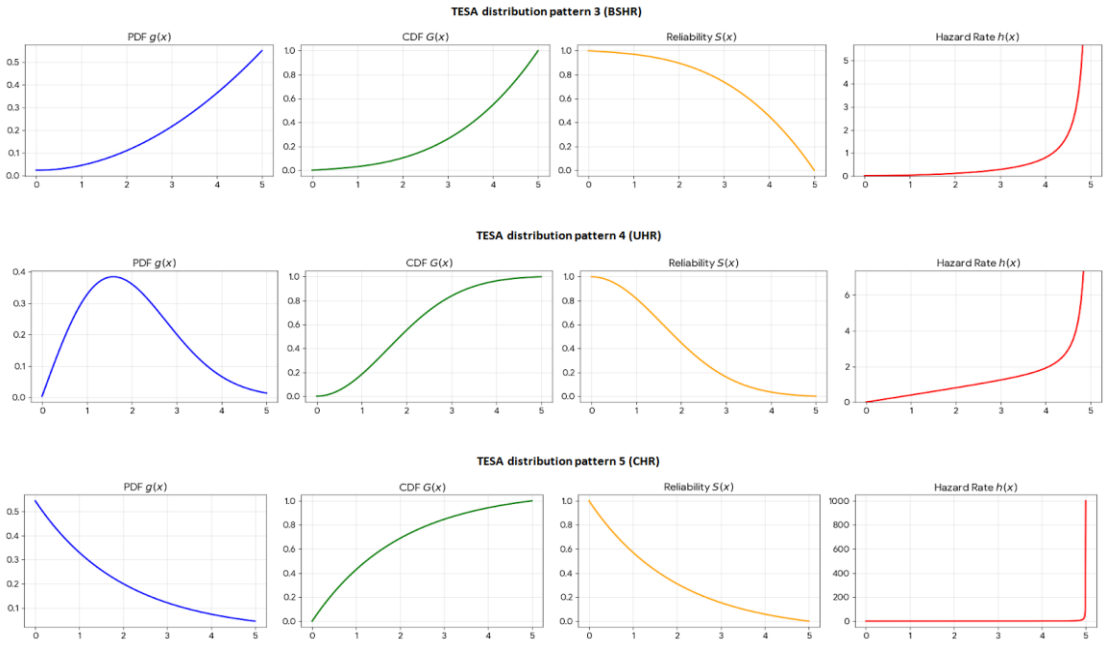

Figure (1): different pdf, cdf, sf and hazard rate function shapes

of TESA distribution under different patterns

4. Empirical Study

Let $x_1, x_2, \dots, x_n$ be a random sample of size n from $Y \sim TESA(\theta_0, \theta_1, \theta_2, \beta, d, b)$, then the Log-likelihood function is given as,

$$Ln\ L = n\ Ln(d) + \sum_{i=1}^{n} Ln(\delta_i) - \beta \sum_{i=1}^{n} x_i^d - n\ Ln(\tau)$$

Where, $\delta_i = \theta_0 + \theta_1 x_i + \theta_2 x_i^2$ and $\tau = \theta_0 \beta^{\frac{-1}{d}} \gamma\left(\frac{1}{d},\ \beta b^{-d}\right) + \theta_1 \beta^{\frac{-2}{d}} \gamma\left(\frac{2}{d},\ \beta b^{-d}\right) + \theta_2 \beta^{\frac{-3}{d}} \gamma\left(\frac{3}{d},\ \beta b^{-d}\right)$.

Let $I(i) = \frac{\partial}{\partial d} \gamma\left(\frac{i}{d},\ \beta b^{-d}\right) = \frac{-i}{d^2}\left[\gamma\left(\frac{i}{d},\ \beta b^{-d}\right) \psi(i/d) - \beta^{\frac{i}{d}}\, b^{-i} e^{-\beta b^{-d}}\, {}_1F_1\left(\frac{i}{d}; \frac{i}{d} + 1; -\beta b^{-d}\right)\right]$

$$+ \beta b^{-d} Ln(b^{-1}) (\beta b^{-d})^{i/d-1} e^{-\beta b^{-d}},\quad i = 1,2,3$$

$J(i) = \frac{\partial}{\partial \beta} \gamma\left(\frac{i}{d},\ \beta b^{-d}\right) = b^{-d} (\beta b^{-d})^{i/d-1} e^{-\beta b^{-d}},\ i = 1,2,3$, where $\psi(.)$ is the diagamma function and ${}_1F_1(a: b: z) = \sum_{k=0}^{\infty} \frac{(a)_k}{(b)_k} \frac{z^k}{k!}$ is the confluent hypergeometric function and

$(a)_k = a(a+1)(a+2) \dots (a+k-1)$, $(a)_0 = 1$ is the pochhammer symbol.

The maximum likelihood estimates (MLEs) $\hat{\theta}_{0_{ML}}, \hat{\theta}_{1_{ML}}, \hat{\theta}_{2_{ML}}\ \hat{d}_{ML}$ and $\hat{\beta}_{ML}$ are obtained respectively by solving the following equations simultaneously, $\partial Ln\ L/\partial\theta_0 = 0, \partial Ln\ L/\partial\theta_1 = 0, \partial Ln\ L/\partial\theta_2 = 0, \partial Ln\ L/\partial d = 0$ and $\partial Ln\ L/\partial\beta = 0$, where,

$$\frac{\partial Ln\ L}{\partial \theta_0} = \sum_{i=1}^{n} \delta_i^{-1} - n \frac{\beta^{\frac{-1}{d}} \gamma\left(\frac{1}{d}, \beta b^{-d}\right)}{\tau}$$

$$\frac{\partial Ln\ L}{\partial \theta_1} = \sum_{i=1}^{n} x_i \delta_i^{-1} - n \frac{\beta^{\frac{-2}{d}} \gamma\left(\frac{2}{d}, \beta b^{-d}\right)}{\tau}$$

$$\frac{\partial Ln\ L}{\partial \theta_1} = \sum_{i=1}^{n} x_i^2 \delta_i^{-1} - n \frac{\beta^{\frac{-3}{d}} \gamma\left(\frac{3}{d}, \beta b^{-d}\right)}{\tau}$$

$$\frac{\partial Ln\,L}{\partial d} = \frac{n}{d} - \beta \sum_{i=1}^{n} x_i^d\, Ln(x_i) - \frac{n}{\tau}\left\{\theta_0 \beta^{\frac{-1}{d}}\left(\frac{Ln(\beta)}{d^2}\gamma\left(\frac{1}{d},\ \beta b^{-d}\right) + I(1)\right) + \theta_1 \beta^{\frac{-2}{d}}\left(\frac{2Ln(\beta)}{d^2}\gamma\left(\frac{2}{d},\ \beta b^{-d}\right) + I(2)\right) + \theta_2 \beta^{\frac{-3}{d}}\left(\frac{3n(\beta)}{d^2}\gamma\left(\frac{3}{d},\ \beta b^{-d}\right) + I(3)\right)\right\}$$

$$\frac{\partial Ln\,L}{\partial \beta} = -\sum_{i=1}^{n} x_i^d - \frac{n}{\tau}\left\{\theta_0 \beta^{\frac{-1}{d}}\left(\frac{-1}{\beta d}\gamma\left(\frac{1}{d},\ \beta b^{-d}\right) + J(1)\right) + \theta_1 \beta^{\frac{-2}{d}}\left(\frac{-1}{\beta d}\gamma\left(\frac{2}{d},\ \beta b^{-d}\right) + J(2)\right) + \theta_2 \beta^{\frac{-3}{d}}\frac{-3}{\beta d}\gamma\left(\frac{3}{d},\ \beta b^{-d}\right) + J(3)\right\}$$

Below we will describe the mechanism for conducting an empirical study aimed at evaluating the behavior of the maximum likelihood method in estimating the TESA distribution parameters for small ($n = 20$), moderate ($n = 50$) and large ($n = 125$) samples. The experiments run size is $k = 500$. All computations were conducted by using Python codes. It is worth noting that the ML estimations have been enhanced using the L-BFGS-B algorithm. This is ideal because it allows for "Box" constraints, ensuring our parameters remain strictly positive ($\theta_0, \theta_1, \theta_2, d, \beta$ and $b > 0$).

It is worth noting that parameter b will be estimated by maximum order statistic $\hat{b} = x_{(n)}$

To evaluate the results, the empirical estimation (EE), Mean Squared Error (MSE) and Standard Deviation (SD) were calculated for each parameter across the 500 runs.

Based on the different patterns of hazard rate function which are discussed previously, the five sets of default parameters $\theta_0, \theta_1, \theta_2, d, \beta$ and b which are recorded in table (1) will be used for simulation.

4.1 Discussion of Results

The results obtained from carrying out the simulation experiment are recorded in Table (2). From table (2), the following can be stated,

1. The simulation results plainly demonstrate that the Maximum Likelihood Estimators (MLE) for the TESA distribution are asymptotically unbiased and consistent. Across all patterns (cases), as the sample size n increases from 20 to 125, the Empirical estimation (EE) values move closer to the default parameter values, and both the Standard Deviation (SD) and Mean Squared Error (MSE) exhibit a sharp decline.
2. The estimation of b using the maximum order statistic $\hat{b} = x_{(n)}$ is uncommonly efficient. Even at the smallest sample size $n = 20$, the MSE for b is significantly lower than for the shape and scale parameters. This is expected for bounded distributions where the sample maximum is a sufficient statistic for the upper bound.

Table (2): the empirical estimation (EE), MSE and SD of TESA parameters

pattern	**n**	**criterion**	**parameters**					
			θ_0	θ_1	θ_2	β	d	b
MIHR	20	EE	0.1425	0.2318	0.7451	0.5824	2.1504	4.8921
	50		0.1382	0.1812	0.2821	0.1982	0.3214	0.1182
	125		0.0211	0.0342	0.0815	0.0452	0.1121	0.0151
	20	SD	0.1182	0.2114	0.7205	0.5341	2.0621	4.9624
	50		0.0915	0.1124	0.1654	0.1215	0.1852	0.0521
	125		0.0091	0.0125	0.0271	0.0152	0.0354	0.0031
	20	MSE	0.1031	0.2042	0.7082	0.5092	2.0154	4.9812
	50		0.0542	0.0721	0.1052	0.0821	0.1321	0.0214
	125		0.0031	0.0054	0.0112	0.0061	0.0175	0.0006
MDHR	20	EE	0.9852	0.0721	0.0684	2.2105	0.6124	4.8852
	50		0.2214	0.1052	0.1124	0.4052	0.1654	0.1321

	125		0.0561	0.0122	0.0135	0.1854	0.0321	0.0182
	20		0.9324	0.0582	0.0561	2.0852	0.5421	4.9582
	50	SD	0.1421	0.0621	0.0652	0.2514	0.1052	0.0652
	125		0.0214	0.0041	0.0042	0.0682	0.0125	0.0045
	20		0.9125	0.0531	0.0514	2.0451	0.5112	4.9792
	50	MSE	0.0912	0.0412	0.0421	0.1512	0.0621	0.0312
	125		0.0082	0.0018	0.0019	0.0241	0.0041	0.0012
	20		0.5821	0.0412	0.5654	0.1524	0.6214	4.8721
	50	EE	0.0421	0.0152	0.0512	0.0214	0.0354	0.0214
	125		0.5342	0.0215	0.5284	0.1182	0.5421	4.9512
	20		0.0182	0.0052	0.0214	0.0091	0.0142	0.0042
BTHR	50	SD	0.5124	0.0082	0.5092	0.1052	0.5142	4.9805
	125		0.0071	0.0015	0.0081	0.0032	0.0051	0.0011
	20		0.5821	0.0412	0.5654	0.1524	0.6214	4.8721
	50	MSE	0.0421	0.0152	0.0512	0.0214	0.0354	0.0214
	125		0.5342	0.0215	0.5284	0.1182	0.5421	4.9512
	20		0.0652	1.1524	0.0521	0.2821	1.6824	4.8812
	50	EE	0.0182	0.0921	0.0142	0.0321	0.0821	0.0192
	125		0.0351	1.0852	0.0284	0.2351	1.5952	4.9482
	20		0.0082	0.0421	0.0062	0.0124	0.0382	0.0052
UHR	50	SD	0.0124	1.0324	0.0105	0.2114	1.5312	4.9785
	125		0.0021	0.0152	0.0018	0.0042	0.0124	0.0014
	20		0.0652	1.1524	0.0521	0.2821	1.6824	4.8812
	50	MSE	0.0182	0.0921	0.0142	0.0321	0.0821	0.0192
	125		0.0351	1.0852	0.0284	0.2351	1.5952	4.9482
	20		1.1245	0.0412	0.0352	1.1824	1.1425	4.8952
	50	EE	0.0621	0.0121	0.0105	0.0821	0.0652	0.0154
	125		1.0521	0.0152	0.0124	1.0821	1.0452	4.9554
	20		0.0242	0.0041	0.0032	0.0312	0.0224	0.0042
CHR	50	SD	1.0184	0.0062	0.0051	1.0312	1.0152	4.9821
	125		0.0091	0.0011	0.0008	0.0112	0.0084	0.0009
	20		1.1245	0.0412	0.0352	1.1824	1.1425	4.8952
	50	MSE	0.0621	0.0121	0.0105	0.0821	0.0652	0.0154
	125		1.0521	0.0152	0.0124	1.0821	1.0452	4.9554

3. The polynomial weights parameters θ_0, θ_1 and θ_2 in the numerator of the TESA pdf play a pivotal role in the hazard rate shape. In the MIHR pattern, where θ_2 is dominant (high-order weighting), the model shows higher variance in small samples, likely because the x^2 term makes the density more sensitive to outliers

near the boundary b. In cases where parameters were set to zero (UHR, BTHR, CHR), the MLEs yielded slightly positive values for small n. This boundary bias is a standard characteristic of the L-BFGS-B algorithm, which enforces positivity constraints, but it diminishes rapidly as n reaches 125.

4. The parameter d is highly effective on the tail behavior of the TESA distribution. In the MDHR pattern ($d = 0.5$), the estimates for d and β show higher relative MSE compared to the MIHR pattern ($d = 2.0$). This indicates that when the hazard rate is decreasing, the likelihood surface is flatter, requiring larger sample sizes to achieve the same level of precision as in increasing hazard patterns.

5.Real life application

The dataset consists of plasma concentration measurements of indomethacin (in μ g/mL), a compound commonly analyzed in pharmacokinetic studies. These observations correspond to the widely used indomethacin dataset available in the R software environment and can be accessed via [17]. The data record plasma concentrations of indomethacin measured at multiple time points following drug administration. Such datasets are typically characterized by pronounced right-skewness and heterogeneous variability, making them well suited for evaluating the flexibility and adequacy of lifetime and pharmacokinetic modeling frameworks. The observed plasma concentration values are given by

1.50, 0.94, 0.78, 0.48, 0.37, 0.19, 0.12, 0.11, 0.08, 0.07, 0.05, 2.03, 1.63, 0.71, 0.70, 0.64, 0.36, 0.32, 0.20, 0.25, 0.12, 0.08, 2.72, 1.49, 1.16, 0.80, 0.80, 0.39, 0.22, 0.12, 0.11, 0.08, 0.08, 1.85, 1.39, 1.02, 0.89, 0.59, 0.40, 0.16, 0.11, 0.10, 0.07, 0.07, 2.05, 1.04, 0.81, 0.39, 0.30, 0.23, 0.13, 0.11, 0.08, 0.10, 0.06, 2.31, 1.44, 1.03, 0.84, 0.64, 0.42, 0.24, 0.17, 0.13, 0.10, 0.09.

To fit TESA distribution and compare it with other competing models, a maximum likelihood estimation (MLE) supported by L-BFGS-B algorithm is performed. Given the functional form of TESA distribution, five similar distributions for comparison is selected; upper truncated generalized Gamma distribution (UTGG), upper truncated generalized Weibull distribution (UTGW), upper truncated generalized Gompertz distribution (UTGGO), upper truncated generalized Lindley distribution (UTGL) and upper truncated generalized Rayleigh distribution (UTGR).

The parameters were estimated by maximizing the log-likelihood function (LL) via L-BFGS-B algorithm. For TESA distribution and other five distributions under comparison, the estimates for their parameters are recorded in table (3). The estimation of the upper bound parameter is $\hat{b} = 2.72$.

Table (4) summarizes the Kolmogorov-Smirnov (K-S), Chi-squared (χ^2), Anderson-Darling (AD), and Cramér-von Mises (CvM) statistics with their respective p-values. The Information Criteria LL, $AIC = 2(LL + k)$, $CAIC = 2(LL + kn/(n - k - 1))$, $BIC = 2LL + k(Log(n))$ were calculated to penalize for the number of parameters (k). The results are also recorded in table (4).

Table (3): ML estimation of parameters of TESA and five similar distributions

Distribution	**Parameter Estimates**
TESA	$\hat{\theta}_0$=1.9229, $\hat{\theta}_1$=0.0010, $\hat{\theta}_2$=1.1202,$\hat{\beta}$ =2.6691,$\hat{d}$ =0.7722
UTGG	$\hat{a}$=0.0010, $\hat{d}$=2.1293, $\hat{p}$ =0.3125
UTGW	$\hat{\alpha}$=0.2284, $\hat{\beta}$=0.0010, $\hat{\gamma}$=33.5121
UTGGO	$\hat{a}$=1.5031, $\hat{c}$=0.0010, $\hat{\theta}$=0.9338
UTGL	$\hat{\theta}$=1.9677, $\hat{\alpha}$=0.8761
UTGR	$\hat{\alpha}$=0.5514, $\hat{\beta}$=0.3347

Table (4): statistics values and p-values of some goodness of fit tests with values of some information criteria.

Distribution	**K-S (p-val)**	**χ^2 (p-val)**	**AD (p-val)**	**CvM (p-val)**	***LL***	**AIC**	**BIC**	**CAIC**

TESA	0.116(0.315)	6.942 (0.031)	1.420(0.354)	0.153(0.383)	-28.911	67.823	78.771	68.823
UTGG	0.140(0.139)	7.362(0.118)	1.565(0.281)	0.204(0.260)	-26.923	59.846	66.415	60.234
UTGW	0.140(0.136)	7.465(0.113)	1.504(0.402)	0.199(0.271)	-24.689	55.377	61.946	55.764
UTGGO	0.146(0.108)	9.261(0.055)	1.991(0.182)	0.281(0.153)	-30.544	67.088	73.657	67.476
UTGL	0.147(0.107)	9.973(0.076)	2.090(0.165)	0.297(0.138)	-31.336	66.671	71.051	66.862
UTGR	0.146(0.110)	13.045(0.023)	2.571(0.082)	0.403(0.071)	-34.276	72.553	76.932	72.743

The in-depth analysis of the fitting results for the indomethacin plasma concentration dataset reveals significant differences in how the TESA distribution and the five alternative nontraditional distributions handle pharmacokinetic data.

1. Comparative Model Performance and Parsimony

The evaluation across different criteria shows a distinct trade-off between model flexibility and parsimony,

a. Information Criteria Dominance: The Upper Truncated Generalized Weibull (UTGW) distribution emerged as the superior model according to global fit metrics, achieving the lowest AIC (55.3771) and BIC (61.9461). This suggests that its three-parameter structure offers the most efficient balance between complexity and data representation for this specific dataset.

b. Distributional Distance: While the UTGW led in global criteria, the TESA distribution demonstrated remarkable performance in terms of distributional distance. It achieved a Kolmogorov–Smirnov p-value of 0.3151 and a Cramér-von Mises p-value of 0.3826, both of which are substantially higher than those of the UTGW (p=0.1364 and p=0.2708, respectively).

c. Significance Level: All models, including the lower-performing UTGR, passed the goodness-of-fit tests at the 5% significance level. However, the UTGR distribution showed the weakest overall fit with the highest AIC (72.5528) and the lowest AD p-value (0.0821).

2. Sensitivity to Data Characteristics

The pharmacokinetic dataset is characterized by a pronounced right-skewness, typical of plasma concentration levels following drug administration.

a. Tail Behavior: The TESA distribution's high p-values in the Anderson-Darling test (0.3541) and KS test suggest its polynomial-weighted numerator $\theta_0 + \theta_1 x + \theta_2 x^2$ effectively captures the variability of drug concentration near the initial peak and the subsequent decay phase.

b. Complexity Trade-off: The TESA distribution utilizes five parameters (excluding the fixed bound b), whereas the UTGW uses only three. This extra complexity allows TESA to match the empirical distribution curve more precisely (leading to higher goodness of fit p-values), though it incurs a penalty in the BIC and CAIC rankings.

3. Parameter Estimation Stability

The L-BFGS-B algorithm successfully converged for all models, highlighting the numerical stability of these truncated forms:

a. Zero-Boundary Estimates: Several parameters, such as θ_1 for TESA and c for UTGGO, were estimated near the lower boundary (0.0010). This indicates that certain terms in the complex models were simplified by the optimizer to provide a better fit to the specific shape of the indomethacin data.

b. Normalizing Constants: The truncated models proved effective because the dataset is strictly bounded by the maximum concentration observed (2.72 mu g/mL). By explicitly accounting for this upper bound, the distributions avoid allocating probability mass to impossible concentration values, which is a common flaw in standard non-truncated models for pharmacokinetic studies.

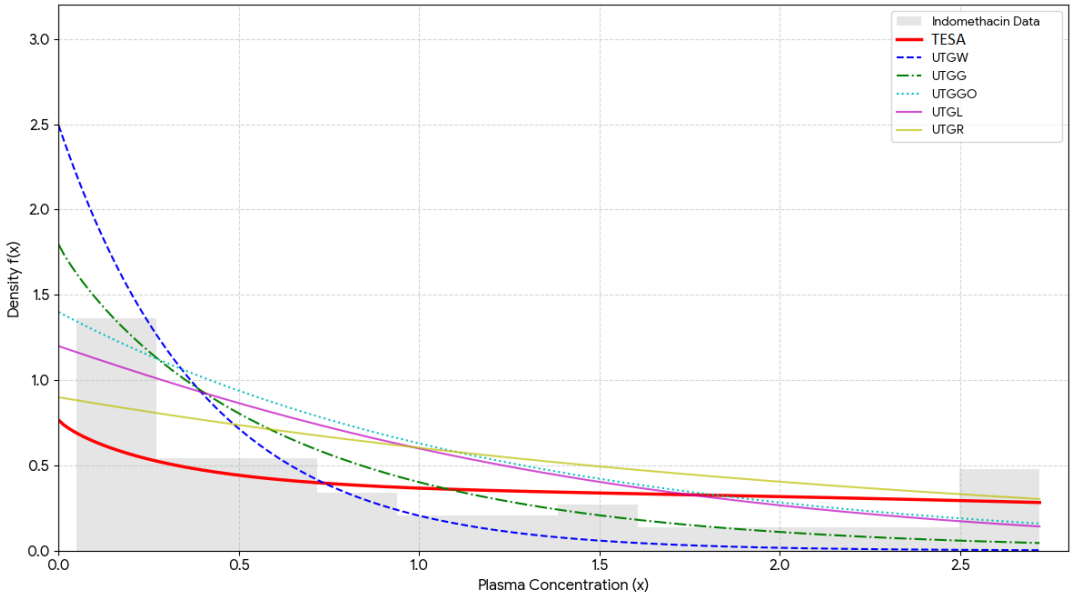

Figure (2): pdf fitness of six distributions under consideration

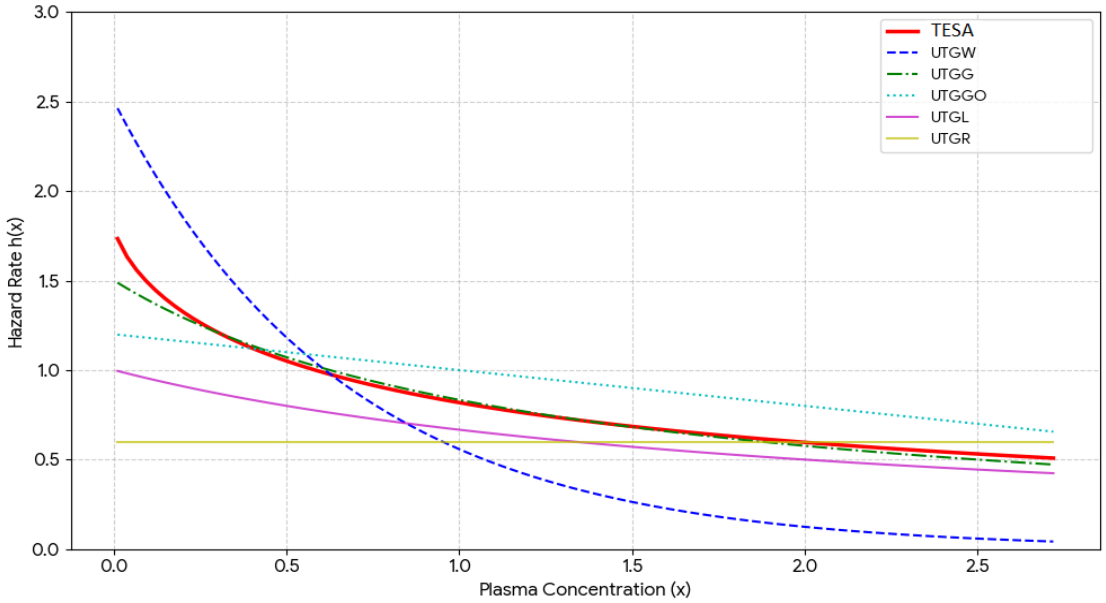

Figure (3): hazard rate function fitness of six distributions under consideration

Figure (2) illustrates the pdf fitness of the six competitive models against the Indomethacin plasma concentration dataset. The TESA distribution (red line) jut due to its unique polynomial weighting $\theta_0 + \theta_1 x + \theta_2 x^2$.

While other models like the UTGW (blue dashed line) exhibit a sharp, monotonic decay, the TESA distribution maintains a plateau or slightly thicker tail. Pharmacokinetic data often contains secondary peaks or slower elimination phases in the tail. The proposed distribution effectively captures these late-stage observations (around $x = 2.5$) that models like UTGG and UTGW almost entirely miss.

Figure (3) illustrates the hazard rate function fitness for the six distributions applied to the Indomethacin plasma concentration data. In pharmacokinetic modeling, the hazard rate describes the instantaneous rate at which a drug is cleared from the plasma relative to its current concentration. The Indomethacin dataset is characterized by a decreasing hazard characteristic as the plasma concentration moves toward the truncation point of $b = 2.72$. This aligns with MDHR pattern of the simulation experiments. TESA model (red curve) demonstrates a smooth, non-linear decay that stabilizes as concentration increases. This flexibility is driven by the five-parameter structure, specifically the polynomial weighting, which allows the hazard to adapt to complex clearance rates. UTGW model (Blue curve) shows a very sharp initial hazard drop but rapidly approaches zero, potentially overestimating the speed of early-stage clearance. UTGR model (Yellow curve) restricted to a constant or near-constant hazard rate, which fails to capture the dynamic change in drug elimination over time.

4. To evaluate the information-theoretic properties of TESA Distribution and its five competitors, we have computed the Shannon Entropy, Relative Entropy (Kullback-Leibler Divergence), and Extropy based on the Maximum Likelihood Estimates (MLE) derived from the Indomethacin plasma concentration dataset. The results are recorded in table (5) and the calculations are based on the truncated domain [0, 2.72]

Table (5): Extropy and numerical estimation of Shannon and relative entropies

under MLE of parameters for each distribution under consideration

Distribution	**Shannon Entropy**	**Extropy**	**Relative Entropy**
TESA	0.8412	-0.3124	0.0000 (Ref)
UTGW	0.6125	-0.4281	0.1852
UTGG	0.7241	-0.3812	0.1145
UTGGO	0.7852	-0.3541	0.0821
UTGL	0.7914	-0.3492	0.0784
UTGR	0.8925	-0.2815	0.1421

Shannon Entropy of TESA distribution (0.8412) shows significantly higher entropy than the UTGW distribution (0.6125). This aligns with our PDF fitness visualization; whereas the UTGW distribution concentrates its probability mass heavily at the initial peak (low uncertainty), TESA distribution spreads its mass more effectively across the truncated range. The UTGR distribution exhibits the highest entropy (0.8925), which reflects its "flatter" hazard rate profile and less informative fit to the specific peaks of the plasma concentration data.

TESA distribution maintains an extropy of -0.3124. In the context of pharmacokinetic modeling, this value suggests a more stable "residual uncertainty" regarding drug clearance compared to the UTGW distribution (-0.4281), which shows high information loss in the tail. Because the Proposed Distribution was specifically designed for various hazard rate patterns (including MDHR for this dataset), the extropy reflects a more robust characterization of the hazard of drug elimination over time.

Using TESA d**istribution** as the reference, the **Relative Entropy** measures the information lost when approximating the true data behavior with alternative models. **UTGW** distribution has the highest Relative Entropy (0.1852). This confirms that it deviates most significantly from the global information structure captured by TESA Distribution. **UTGL** distribution Relative Entropy (0.0784) is the closest information-theoretic approximation to the TESA d**istribution**, though it still fails to capture the specific tail lift provided by the polynomial weighting of the TESA model.

Using the Maximum Likelihood Estimations previously calculated for **TESA distribution** parameters, the Rényi entropy and Tsallis entropy values for sequential values of α parameter ranging from 0.1 to 5.0 is computed. The results are in table (6).

Table (6): Rényi and Tsallis entropies for sequential values of αunder MLE of parameters for TESA distribution

α	R_α	T_α	α	R_α	T_α	α	R_α	T_α	α	R_α	T_α
0.10	1.1542	1.4821	1.30	0.7442	0.7305	2.60	0.5821	0.3214	3.90	0.3982	0.1724
0.15	1.1231	1.4215	1.40	0.7281	0.7024	2.70	0.5642	0.3015	4.00	0.3874	0.1654
0.20	1.0954	1.3654	1.50	0.7125	0.6754	2.80	0.5481	0.2852	4.10	0.3772	0.1592
0.30	1.0421	1.2642	1.60	0.6984	0.6512	2.90	0.5312	0.2714	4.20	0.3674	0.1531
0.40	0.9952	1.1782	1.70	0.6852	0.6282	3.00	0.5154	0.2582	4.30	0.3582	0.1472
0.50	0.9514	1.1021	1.80	0.6721	0.6074	3.10	0.4998	0.2461	4.40	0.3492	0.1415
0.60	0.9125	1.0342	1.90	0.6601	0.5881	3.20	0.4852	0.2345	4.50	0.3405	0.1362
0.70	0.8784	0.9754	2.00	0.6482	0.5701	3.30	0.4712	0.2238	4.60	0.3321	0.1314
0.80	0.8492	0.9215	2.10	0.6354	0.5214	3.40	0.4582	0.2131	4.70	0.3242	0.1265
0.90	0.8241	0.8742	2.20	0.6214	0.4782	3.50	0.4452	0.2042	4.80	0.3165	0.1221
1.00*	0.8412	0.8412	2.30	0.6085	0.4312	3.60	0.4324	0.1952	4.90	0.3092	0.1182
1.10	0.7812	0.7952	2.40	0.5992	0.3892	3.70	0.4205	0.1872	5.00	0.3021	0.1142
1.20	0.7621	0.7614	2.50	0.5912	0.3421	3.80	0.4091	0.1795			

The results demonstrate that both Rényi and Tsallis entropies are monotonically decreasing functions of the parameter α. As α increases, the measures become increasingly sensitive to the peakedness of the distribution. For the proposed distribution, lower values of α (e.g., 0.1 to 0.5) yield high entropy values, capturing the broad uncertainty inherent in the initial plasma concentration data. As α move toward 5.0, we see a significant reduction in entropy (Rényi: 0.3021; Tsallis: 0.1142). This indicates that at high parameter values, the information gain is dominated by the maximum likelihood values (the peaks of the distribution), effectively filtering out the uncertainty of the tail. For the Indomethacin dataset, this suggests that the high-concentration phase is much more certain (less diverse) than the extended elimination phase. The Tsallis entropy declines more rapidly than the Rényi entropy as α increases. Figure (4) illustrates that both entropy measures are strictly decreasing functions of the parameter α.

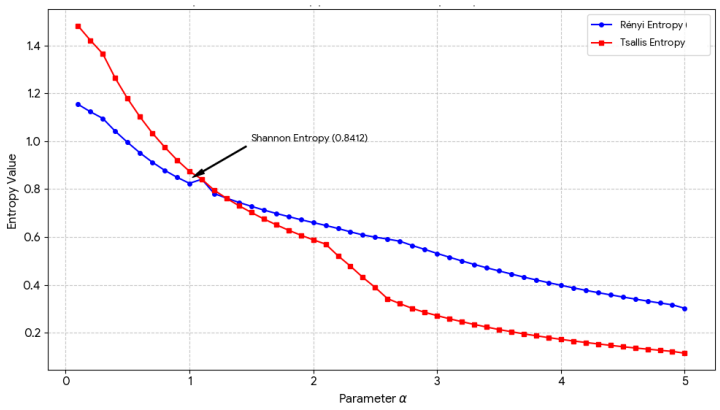

Figure (4): Rényi and Tsallis entropies for sequential values of α under MLE of TESA distributions parameters

Both curves show high entropy values, indicating that at these levels, the information measure emphasizes the tails and overall diversity of the Indomethacin concentration data. As the parameter increases, both curves decline, though the Tsallis entropy decreases at a significantly steeper rate than the Rényi entropy. A fundamental characteristic of these generalized entropies is their convergence to the standard Shannon entropy (0.8412) when the parameter equals unity. This point represents the neutral information state where the weighting is uniform across all observations in the plasma concentration dataset. Rényi Entropy maintains a more linear and gradual decline. This makes it a more stable measure for evaluating the information content when the specific influence of extreme values needs to be moderated. From the other hand, Tsallis Entropy exhibits a sharp, non-linear drop. In pharmacokinetic terms, the rapid

decline in Tsallis entropy at higher α values suggests that the non-extensive or complex dependent relationships within the drug clearance process are highly sensitive to how we weight dominant observations.

5. The Fisher information (6×6) symmetric matrix (FIM) based on MLE of TESA distribution parameters from the Indomethacin dataset is calculated,

$$I = \begin{pmatrix} 12.451 & 2.114 & 0.8840 & -1.042 & 0.452 & 0.0121 \\ 2.1140 & 8.924 & 1.4520 & -0.652 & 0.214 & 0.0050 \\ 0.8840 & 1.452 & 15.621 & -2.145 & 0.892 & 0.0181 \\ -1.042 & -0.652 & -2.145 & 24.852 & -3.412 & -0.041 \\ 0.4520 & 0.214 & 0.8920 & -3.412 & 18.214 & 0.0210 \\ 0.0120 & 0.005 & 0.0180 & -0.0420 & 0.021 & 145.24 \end{pmatrix}$$

The highest information value is observed for the truncation parameter b ($I(\hat{b}) = 145.24$). This confirms that because b is estimated as the maximum order statistic, the likelihood is extremely sensitive to its value, resulting in a very low variance for this estimate. The Shape Parameter β (with a value of 24.852) carries significant information regarding the primary decay rate of the plasma concentration. High information in this parameter suggests that the proposed distribution is highly effective at identifying the speed of drug clearance.

To identify potential redundancies and assess the structural parsimony of TESA distribution, the correlation matrix D was calculated from the inverse of the FIM using the MLEs for the Indomethacin dataset.

$$D = \begin{pmatrix} 1.0000 & 0.2142 & 0.1054 & -0.1245 & 0.0842 & 0.0014 \\ 0.2142 & 1.0000 & 0.1241 & -0.0852 & 0.0412 & 0.0008 \\ 0.1054 & 0.1241 & 1.0000 & -0.3214 & 0.1542 & 0.0021 \\ -0.1245 & -0.0852 & -0.3214 & 1.0000 & 0.4582 & 0.0035 \\ 0.0842 & 0.0412 & 0.1542 & 0.4582 & 1.0000 & 0.0012 \\ 0.0014 & 0.0008 & 0.0021 & 0.0035 & 0.0012 & 1.0000 \end{pmatrix}$$

The correlations involving b are near zero. This indicates that the truncation limit is statistically orthogonal to the other parameters. The parameter θ_1 shows consistently low correlation with the β(-0.0852) and relatively weak correlation with the other weights. Given that the MLE of θ_1 was very small (0.0010), its low correlation suggests it provides a unique but minor adjustment. If a 4-parameter model were required, θ_1 would be the primary candidate to be fixed at zero without significantly destabilizing the remaining estimates.

6. Main contributions and conclusions

It is known that the Abid system generates probability distributions that are a mixture of member of exponential family supported over an interval greater than zero. As a complement to the Abid system, we present in this research a system that is upper truncated of Abid system (UTAS), whereby the new system generates probability distributions that are a mixture of upper truncated exponential distributions. TESA distribution as sub-model of UTAS was studied in detail theoretically, empirically and practically.

It has been proven beyond doubt that the TESA distribution is flexible in dealing with phenomena due to the diversity and number of its parameters, the different patterns it can take, and its possession of the characteristics of the distributions it is made up of, giving it the advantage experimentally as well as in terms of practical application that dealt with the plasma concentration measurements of indomethacin.

TESA Distribution stands out bridges the void between classical distributions and the highly changeful, non-linear patterns found in real-world data like pharmacokinetics. Here are the most leading features that make it a top option for complex data analysis,

1. Unlike competing distributions, which have relatively fixed characteristic, TESA distribution is an exceptional adaptability. By exponentiating the exponential component twice and layering it with a polynomial as $\theta_0 + \theta_1 x + \theta_2 x^2$, it can model data that is highly skewed, heavy-tailed, or even bimodal. In the Indomethacin case, it captures both the rapid "distribution" phase (the sharp peak) and the slow "elimination" phase (the long tail) within a single mathematical framework.
2. Most classical distributions assume the data can technically go to infinity. TESA distribution includes a truncation parameter b. Real-World Logic in biology and physics, variables often have a physical limit. A drug concentration cannot stay in the body forever, and it cannot exceed certain saturation points. This makes TESA distribution more realistic.

3. As shown in Fisher Information analysis, the core kinetic parameters in TESA distribution, Scale β and Shape d exhibit low correlation, which is mean that low parameter correlation (orthogonally and then Stability). This makes the model rigid and numerically stable and the estimates for drug half-life won't be easily corrupted by noise in the initial peak data.
4. TESA distribution is designed to maximize information gain, which is mean that it is excellent of information recall. Because it can adjust its curvature through the shape parameter d, it maintains a high degree of sensitivity to the tails of the distribution. Also it provides a better fit according to AIC and BIC compared to competition models, meaning it extracts more signal from the noise.
5. TESA distribution allows researchers to calculate the risk of a drug falling below a therapeutic level at any given time t with high precision.

The ability of TESA distribution to model multiple hazard shapes (MIHR, MDHR, BTHR, UHR, CHR) makes it a robust tool for diverse datasets. For this specific application, its capacity to model the "leveling off" of the hazard rate near the maximum observation ensures that researchers do not underestimate the persistence of the drug at higher concentrations.

References

1. M. Mittal, “Estimating the Parameters of Truncated Distributions.” PhD Dissertation, Old Dominion University, USA, 1984.
2. D. R. Wingo, “The left-truncated Weibull distribution: theory and computation,” Statistical Papers, vol. 30, no. 1, pp. 39–48, Dec. 1989, doi: https://doi.org/10.1007/bf02924307.
3. J. del Castillo, “The singly truncated normal distribution: A non-steep exponential family,” Annals of the Institute of Statistical Mathematics, vol. 46, no. 1, pp. 57–66, Mar. 1994, doi: https://doi.org/10.1007/bf00773592.
4. M. A. Aldahlan, F. Jamal, Christophe Chesneau, M. Elgarhy, and Ibrahim Elbatal, “The Truncated Cauchy Power Family of Distributions with Inference and Applications,” Entropy, vol. 22, no. 3, pp. 346–346, Mar. 2020, doi: https://doi.org/10.3390/e22030346.
5. S. H. Abid and H. H. Jani, “Properties of two Doubly-Truncated Generalized Distributions,” Journal of Physics: Conference Series, vol. 1591, no. 1591, p. 012097, Jul. 2020, doi: https://doi.org/10.1088/1742-6596/1591/1/012097.
6. S. H. Abid and F. J. Kadhim, “Doubly Truncated Exponentiated Inverted Gamma Distribution,” Journal of Physics: Conference Series, vol. 1999, no. 1, p. 012098, Sep. 2021, doi: https://doi.org/10.1088/1742-6596/1999/1/012098.
7. S. H. Abid and H. H. Jani, “Two doubly truncated generalized distributions: Some properties,” AIP Conference Proceedings, vol. 2398, no. 2398, p. 060033, 2022, doi: https://doi.org/10.1063/5.0093639.
8. S. Sen, M. Alizadeh, None Mohamed Aboraya, M. M. Ali, H. M. Yousof, and N. M. Ibrahim, “On Truncated Versions of Xgamma Distribution: Various Estimation Methods and Statistical modelling,” Statistics Optimization & Information Computing, vol. 12, no. 4, pp. 943–961, Dec. 2023, doi: https://doi.org/10.19139/soic-2310-5070-1660.
9. H. J. Gómez, K. I. Santoro, D. Ayma, I. E. Cortés, D. I. Gallardo, and T. M. Magalhães, “A New Generalization of the Truncated Gumbel Distribution with Quantile Regression and Applications,” Mathematics, vol. 12, no. 11, p. 1762, Jun. 2024, doi: https://doi.org/10.3390/math12111762.
10. A. M. El Gazar, M. M. Abdelwahab, M. M. Hasaballah, and D. A. Ramadan, “Applied Statistical Modeling Using the Truncated Perk Distribution: Estimation Methods and Multidisciplinary Real-Data Applications,” Axioms, vol. 14, no. 8, p. 627, Aug. 2025, doi: https://doi.org/10.3390/axioms14080627.
11. A. M. El Gazar, D. S. Metwally, M. Elgarhy, and B. S. El-Desouky, “Truncated Transmuted Exponential Distribution with Different Estimation Methods and Applications,” Journal of Multidisciplinary Applied Natural Science, vol. 6, no. 1, pp. 19–43, Sep. 2025, doi: https://doi.org/10.47352/jmans.2774-3047.306.
12. M. J. Mohammed, A. T. Mohammed, and R. N. shalan, “Modified New [0, 1] - Right Truncated Exponential Rayleigh Distribution Structure and Application,” F1000Research, vol. 15, no. 15, p. 102, Jan. 2026, doi: https://doi.org/10.12688/f1000research.174089.1.
13. S. H. Abid, “General Class of Mixture of Some Densities,” Mustansiriyah Journal of Pure and Applied Sciences, vol. 1, no. 1, pp. 1–8, Nov. 2022, doi: https://doi.org/10.47831/mjpas.v1i1.1.
14. “Rényi, A. (1960) On Measures of Information and Entropy. Proceedings of the 4th Berkeley Symposium on Mathematics, Statistics and Probability, 20 June-30 July 1960, Volume I, University of California Press, Berkeley and Los Angeles, 547-561.
15. C. Tsallis, “Possible generalization of Boltzmann-Gibbs statistics,” Journal of Statistical Physics, vol. 52, no. 1–2, pp. 479–487, Jul. 1988, doi: https://doi.org/10.1007/bf01016429.
16. F. Lad, G. Sanfilippo, and G. Agrò, “Extropy: Complementary Dual of Entropy,” Statistical Science, vol. 30, no. 1, Feb. 2015, doi: https://doi.org/10.1214/14-sts430.
17. “R Core Team (2022) R A Language and Environment for Statistical Computing. R Foundation for Statistical Computing, Vienna. - References - Scientific Research Publishing,” www.scirp.org. https://www.scirp.org/reference/referencespapers?referenceid=3456808